IJE TRANSACTIONS A: Basics Vol. 29, No. 10, (October 2016) 1431-1440

International Journal of Engineering

Journal Homepage: www.ije.ir

On Numerical Investigation of Non-dimensional Constant Representing the Occurrence of Secondary Peaks in the Nusselt Distribution Curves

S. Mohd Umair, N. Parashram Gulhane*

Department of Mechanical Engineering, Veermata Jijabai Technological Institute, Mumbai

PAPER INFO

Paper history:
Received 07 July 2016
Received in revised form 13 August 2016
Accepted 03 September 2016

Keywords:
Heat Transfer
Heat Sinks
Nusselt Number
Computational Simulations
Secondary Peaks

ABSTRACT

The characteristic study of heat dissipation rate is done with by numerically evaluating the radial distribution of Nusselt magnitudes over a flat plate. These profiles are reported for various injection and geometric parameters in the present research. A very contagious look towards these profiles shows the occurrence of secondary and localized rise. However these local rises are observed provided the Nusselt profiles are accurately predicted. To achieve this, the present research takes an effort in numerically simulating a computational domain, analogous to actual experimental conditions. The computational simulations at lower nozzle-target spacing and higher impinging velocity revels the occurrence of secondary rise in Nusselt profiles. A very less light is observed in determining the exact cause and the intervening range for the occurrence of such peaks in the profiles. Looking into this, the current research focuses on the determination of the critical constant and its magnitude within which these peaks exist in the profile. The non-dimensional constant representing the critical magnitude is defined as a ratio of diameter based Reynolds number with nozzle - target spacing (Z/d). A very judicious look towards the velocity contour conveys the occurrence of turbulence flow in near wall region to be responsible for the secondary rise in heat transfer rate.

***doi**: 10.5829/idosi.ije.2016.29.10a.14*

NOMENCLATURE

Re	Reynolds number.	p	Static pressure (N/m^2)	a	Ambient condition	conv	Convection rate of heat	f	External force per unit mass (m/s^2)
Pr	Prandtl number.	V	Mean velocity (m/s)	b	Base plate.	rad	Radiation heat transfer	τ	Shear tensor (N/m^2)
Nu	Nusselt number.	S	Source term	s	Steady state.	avg	Average	ε	Emissivity
Q	Heat input (W/m^2)	Z	Nozzle-target spacing (m)	z	Jet to target spacing			σ	Stefan-Boltzmann's constant (W/m^2-K^4)
r	Radial distance (m)	C	Non dimensional constant	m	mass generation			ρ	Density of air (kg/m^3)
t	Geometric thickness (mm)			cond	Conduction rate of heat				

1. INTRODUCTION

Heat transfer augmentation using steady/pulse jet impinging on flat plate finds abundant applications in material processing industries, drying technologies and electronic packaging system. As far as the efficiency of these appliances is concerned, cooling rate due to impingement of air jet plays a bottom line role. Application of air jet impingement in cooling of gas turbine blades and robotics application is the upcoming challenge of the impending universe. In this attempt, the noisy components like fans and blowers can be replaced. Cooling of these appliances using air jet gives

*Corresponding Author's Email: *u.i.siddiqui@gmail.com* (S. Mohd Umair)

Please cite this article as: S. Mohd Umair, N. Parashram Gulhane, On Numerical Investigation of Non-dimensional Constant Representing the Occurrence of Secondary Peaks in the Nusselt Distribution Curves, International Journal of Engineering (IJE), TRANSACTIONS A: Basics Vol. 29, No. 10, (October 2016) 1431-1440

comparatively higher cooling rate as that achieved by conventional cooling practices. Generally, the rate of cooling is measured by calculating Nusselt number. This is the non-dimensional parameter which represents the magnitude of convective heat transfer. As far as cooling of the heat sink by impingement of air jet is concerned, accurate calculation of area averaged and local Nusselt number becomes a challenging task. This is more difficult when the distribution curve becomes non-uniform. This non- uniformity in Nusselt distribution curve arises due to the presences of secondary peaks. This unpredictable rise occurring in the wall jet region mainly depends upon nozzle - target spacing and impinging Reynolds number (Re_z).

The basic research for studying the temperature distribution due to air jet impingement is mostly carried out experimentally. The common experimental setup used basically consists of a target plate and an air impinging nozzle. The air inside the nozzle is being carried at specified Reynolds number and impinges over the hot target surface. Thermocouples mounted over the plate enable the local temperature measurement. This is how the temperature distribution curve is plotted over the radial distance on the target surface. However, it is observed that extensive research is carried out in the field of the air jet impingement cooling mechanism by plotting local Nusselt number distribution curve over a flat plate and modified target surfaces. Hani and Suresh [1] compared the heat transfer coefficient for unpinned and pinned surface in the presence of single and multi-jet by varying Reynolds number, nozzle-target spacing and diameter of the nozzle. The graphical justification showed the strong dependency of heat transfer coefficient on the air flow rate of the impinging jet. 60% increment in heat transfer rate was obtained for pinned surface in presences of multi-jet with that compared to unpinned ones. Also, the stagnant point Nusselt number was correlated as $Nu=3.361\ Re^{0.724}\ Pr^{0.4}\ (D_e/d)^{-0.689}\ (S/d)^{-0.10}$. Suresh and Vincent [2] further took an effort in determining the local heat transfer coefficient across the radial distance of pin fin surface by varying H/d and Reynolds number. The comparison was made between the multi jets impinging array of 9×1.59 mm and 4× 3.18 mm with a single jet. 20% increment in heat transfer coefficient for 4×3.18 mm over 9×1.59 mm was observed. The dominancy of multi-jet in heat transfer coefficient observed was due to intermediate peaks in Nusselt distribution curve. These intermediate/ secondary peaks seem to shifts toward the center as a result of which the Nusselt distribution curve becomes flattened. This happens with a simultaneous increase in Reynolds number and decrease in a jet to target spacing. Furthermore, the stagnant point Nusselt number in terms of impinging and geometric parameter was correlated as $Nu_s=0.161\ Re_s^{0.707}\ Pr^{0.4}\ (H/d)^{-0.104}$. On the other hand, Yoshisaburo et al. [3] determined the effect of the jet to the target and inter jets spacing on heat transfer rate using thermionic liquid crystal. As far as impingement over a flat plate is concerned, extensive research is carried with a wide range of impinging and geometric parameter in order to study the Nusselt distribution curve. Not only that the use of multi-jet in combination with flat plate has been vastly studied, but the calculation of area average Nusselt number over the surface and its significant effect due to the presences of secondary peak is not being studied yet.

Lytle and Webb [4] performed an experimental study for heat transfer distribution over a flat plate at low Z/d spacing, in order to capture the secondary peaks. At low Z/d spacing, two peaks apart from that occurring at stagnation point was observed due to accelerated radial flow just exit to the tube. The secondary peaks in Nusselt distribution curves were being justified due to the termination of flow within the length of the potential core. Due to the destroying of the potential core, turbulence gets induced inside and outside the stagnation region resulting in thinning of the boundary layer. As a result of which secondary peaks occur and heat transfer increases. Also, the local radial distances at which these peaks exist were examined in terms of Reynolds number. On the other hand, Kyo and Sung [5] experimentally determined the effect of pumping power on heat transfer distribution over a flat plate under steady air jet impingement. Experiments were performed at nozzle-target spacing equal to, and less than one. A remarkable peak in Nusselt distribution curve far away from stagnation point at r/d=0.125 with impinging Reynolds number of 5100 was observed. The above research was conducted on the experimental setup in which the effort and time required are enormous. Furthermore, to demonstrate huge sets of experimental reading at different varying parameters, experimental analysis becomes a less powerful tool. Hence, the need arises for solving the heat transfer augmentation problem via numerical analysis. Ganamatayya and Santosh [6] studied the effect of L/d ratio on Nusselt number distribution curve by varying nozzle-target spacing from 0.5 to 12 times the diameter. The study was achieved by solving the problem of air jet impingement over a flat plate numerically in commercial computational software (FLUENT). For computing, this problem V2-f turbulence model was used. Jun and Jiin [7] on the other hand studied heat transfer distribution over a flat plate by impinging the mixture of water and particles of aluminum oxide. Numerical analysis was carried at different concentrations of nano-fluids, Reynolds number and Z/d. The results of simulation revealed a strong dependence of concentration ratio of nanofluids on local heat transfer coefficient. In order to consider the turbulence and mixing regime, Jun – Bo Huang and Jiin–Yuh Jang [7] selected SST turbulent model. Furthermore, secondary peaks in the Nusselt distribution curve was observed at H/d=2 and Reynolds

number of 2000 with the magnitude being more prominent at higher concentrations. The study fails in justifying the physical significance behind the occurrence of these peaks.

Gorji et al. [8] examined ten types of eddy viscosity turbulence models in predicting the flow behavior for ramp up flow. Three ramps up the flow with different accelerations were chosen for experimentation. Turbulent shear stress transport was captured with respect to the change in flow rate while a delay in capturing of dynamic turbulent shear stress by the current computational model was observed. Hence the results of different thermo physical parameters in transition region seem to be inaccurately plotted. On the other hand, gamma theta model proposed by Robin and Florain [9] proves to capture these delays far more accurately. This is achieved by invoking an intermediary term at every iteration, the values for which ranges from zero to unity inside the boundary layer. Paul et al. [10] completely calibrated the gamma theta model by coupling it with SST turbulence model. This calibration work was carried out by numerically analyzing the flat plate and airfoils at different flow rates. As far as the capability of this coupled (SST + Gamma – Theta) turbulence model in commercial computing software is concerned, it was observed to capture the transition flow regime and corresponding heat interaction very accurately.

Angioletti et al. [11] visualized the flow contour by laterally impinging air jet over a flat plate with the help of PIV. In this study k - ε, k - ω and SST turbulence models were examined for flow analysis and results for velocity contour were plotted. Looking into the velocity contour, it was observed that the flow of air jet before striking the plate was found to spread. This happens due to entrainment of fresh air which cannot be noticed in PIV plots. This effect was found to be well captured by SST turbulence model which gave the most accurate prediction of the realizable flow field. Also, the stagnant point was accurately seen to be configured. On the other hand, Alenezi et al. [12] compared k-ε, k-ω and SST turbulence models for analyzing the flow development inside a narrow trench at Mach number of 1. The study incorporated the computation using commercial software CFX. As a result of computation, SST turbulence model showed quite accurate development of flow field and thermal regions. Khameneh et al. [13] reported an accurate prediction of single phase laminar flow in micro-channel using Fluent solver. Also, the forced convection heat transfer was accurately predicted. Here the physics of area average Nusselt number was of great concern. Sundaram and Venkatesan [14] analyzed the flow field over the pin fin surface using RNG turbulence model and reported an error of 0.3% in the evaluation of average temperature. On the other hand, Khoshravan and Soleimani [15] reported the interaction of radiation and conduction rate of heat transfer on natural convection. The distribution of local Nusselt magnitude was found to be far effected due to the radiation heat loss. Above all, Rostamzadeh et al. [16] reported the dependency of impinging Reynolds number on convective heat transfer rate. Also, an empirical relation was proposed for evaluating the magnitude of Nusselt number for W-shaped tube.

Hence it can be concluded that the score of research in the area of secondary peaks occurrence in Nusselt distribution curve, its physical reasoning and the promising condition for its occurrence is very less studied. No doubt Katti and Prabhu [17] came forward in with this issue and extensively plotted local Nusselt distribution curve over the flat plate at lower nozzle - target spacing. Most of the reported Nusselt curve contains secondary peaks. Here the impingement of air was carried out at Reynolds number ranging from 12,000 to 28,000 with Z/d ranging from 0.5 to 8. Katti and Prabhu [17] observed the secondary peaks for the first time at Z/d=0.5 and concluded the existence of transition region in flow regime at target surface to be responsible for it. Furthermore, the ranging condition for the existences of secondary peaks in terms of Z/d and Reynolds number remains incompletely described. Also, the condition signifying the occurrence of a secondary peak in terms of the nozzle-target spacing and impinging Reynolds number was not explained clearly. The present work targets the implementation of the current problem in commercial simulating software (ANSYS CFX) with optimal grid size. The optimal size of the grid geometry is the one which consumes the least computational time and cost. This is achieved without any compromise in the accuracy of computed parameters. However, different trials of mesh size are conducted in the present work to report the most optimistic one. After a particular trial (mesh size), the computed parameters do not show any deviation from previous one. This is known as optimal grid geometry. Also, an appropriate turbulence model capable of accurately predicting the realizable flow regime is signified and implemented in the present study. However, the key aim of the present research is to construct a non-dimensional parameter which decides the occurrence of a secondary peak in Nusselt distribution profile. Not only this, a critical magnitude of the corresponding non-dimensional number is being proposed. The benefit of this critical magnitude helps in deciding the occurrence of a secondary peak in Nusselt profile. Also, the corresponding physical reasoning for their occurrence is being well justified.

2. EXPERIMENTAL SETUP

The current setup avails the variation in impinging Reynolds number, nozzle-target spacing, heat input and the type of target surface used for impingement.

The basic experimental setup to measure heat transfer through the aluminum flat surface (100mm × 100mm) consists of inlet blower of capacity 0.05 m^3/s which pumps the fresh atmospheric air into an aluminum body nozzle. Also, with the help of rotating handle mounted on a threaded shaft which is further riveted to air plenum (body containing nozzle), nozzle - target spacing can be adjusted (Figure 1). The impinging velocity of air jet is measured with the help of a hot wire anemometer (C.A. 1226). An error of 0.05 m/s is observed at the target surface while measuring the velocity. Electric heater mounted on the bottom side of the surface (Heat sink), ensures constant temperature throughout the surface body. Since it is very difficult to maintain the perfect contact of heater and flat surface, hence an uncertainty of ± 6.25% (1–1.2 Watts) occurs during heating the target surface. Data Acquisition system (DAQ) ensures the recording of instantaneous and local temperature of the heat sink. This is achieved with the help of four T-type thermocouples diagonally mounted on the target surface. The thermocouple carries a precision of $\pm 0.1^o$ C, with a measuring range of 0^o C – 450^o C. The response time for the measurement is 0.1 sec.

Above all, the most important concern is energy balance

$$Q = Q_{cond} + Q_{conv} + Q_{rad} \quad (1)$$

$$Q_{cond} = K\left(\frac{\Delta T}{t}\right) \quad (2)$$

$$Q_{rad} = \varepsilon \sigma \left(T_b{}^4 - T_a{}^4\right) \quad (3)$$

Here, the radiation component of heat loss at 50^o C of steady temperature for base plate rounds to 8.39 W/ m^2 (Equation (3)). Since an aluminum sheet is used as a target surface, the corresponding emissivity for the magnitude for aluminum surface is selected as 0.032 for the present calculation [18]. However, the heat loss due to radiation and natural convection from back surface is not considered, since the back side of the target surface is exposed to constant heat flux input (1500 W/m^2). Still, katti and Prabhu [17] estimated these components of back side loss and concluded a very less magnitude. However, for the present work, the magnitude of radiation loss in comparison with the supplied heat input (1500 W/m^2) approximates to 0.01%.

Looking into the conduction component of heat loss, the geometric thickness (t) which happens to be in the denominator of Equation (2), possesses a much smaller magnitude. This may boost up the conduction heat lost. However, the magnitude (ΔT) which represents the temperature difference between the top and bottom surface of target heat sink is examined to be very small. This is due to the low value of geometric thickness possessed by the target surface. No doubt, the corresponding heat lost due to conduction approximates to 33.4 W/m^2 (Calculated using Equation (2)). Hence, around 2.2% of heat loss occurs due to conduction from side wall. This is very small in comparison with supply heat input (1500W/m^2). However, the heat flux input during the impingement of air varies by 0.125%, even after the attainment of steady temperature profile. Hence, the evaluated temperature carries an uncertainty of 0.125%. Also the corresponding heat transfer coefficient reported is based on pure convection, while around 3% of heat loss occurs due to conduction and radiation. Above all, the limited number of thermocouples used in the present setup ceases an inaccurate prediction of Nusselt profile. Hence, computational simulations are being suggested.

3. METHODOLOGY

The rate of cooling for the flat aluminum plate is measured with the help of forced convective heat transfer coefficient at steady state as shown in Equation (4).

$$h = \frac{Q}{A \times (T_b - T_a)} \quad (4)$$

Nusselt number is the non-dimensional parameter which measures the ratio of the magnitude of heat convected due to impinging air jet to the heat conducted as shown in Equation (5).

$$Nu = h \times \frac{d}{k_a} \quad (5)$$

As far as the time and energy for performing the experiments are concerned, it seems to be consuming a huge time in order to give the steady temperature distribution over the plate. In order to compensate for this physical time and energy, numerical simulations are being suggested and carried out in the present work. The numerical method commands the continuity (Equation (6)), momentum (Equation (7)) and energy equation to be solved simultaneously in order to develop the flow regime and plot the corresponding heat interaction.

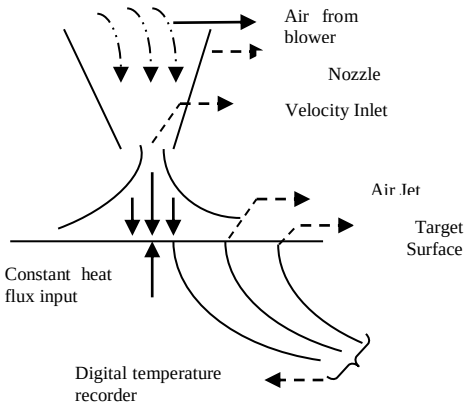

Figure 1. Schematic layout of experimental setup

This is achieved by simulating the geometry in commercial simulating software, ANSYS CFX. The computational simulations are carried out through second order upwind scheme with standard value of turbulence intensity (1-3%) and Prandtl number (0.7).

$$\frac{\partial \rho}{\partial t} + \nabla(\rho.\vec{v}) = S_m \quad (6)$$

$$\frac{\partial \vec{v}}{\partial t} + \nabla(\rho.\vec{v}.\vec{v}) = -\nabla p + \nabla.\overline{\overline{\tau}} + \rho\vec{g} + \vec{f} \quad (7)$$

While the convergence criterion for every computed parameter is taken to be 10^{-8}. No doubt the temperature profile is the one to converge earliest. However, the computational time required for the convergence, approximates to 2 hours. Taking into consideration the computational time and cost, a 2-D axis symmetric model was developed as seen in Figure 2. During the process of simulation, it is assumed that the flow of air is incompressible and single phase. While the thermo-physical and flow property of target surface and air jet remains constant. The 2–D axis symmetric model consist of nozzle and target plate along with computational domain is shown in Figure 2. The geometric model is designed in commercial design modeler of ANSYS CFX. The geometry is divided into two computational domains of air and solid. The solid domain comprises of aluminum plate over which the jet impinges. Further, the designed model is imported into mesh deign modeler for the purpose of meshing. Generally, tetrahedron meshing with flexible growth rate and edge size is performed in order to discrete the computational domain. During the process of meshing, the edges containing air jet and base plate are intentionally divided into more number of divisions as compared to the rest. This increases the grid density and population in the region containing air jet and base plate.

The present axis symmetric geometry as shows in Figure 2 is solved in the commercial solver of ANSYS CFX. The computational domain is classified into two categories, fluid and solid (plate) domain. The exit wall of the nozzle is provided with velocity inlet with a turbulence intensity of 1–3%, as justified by Sajad et al. [19]. On the other hand, the opening of domain in atmosphere is set to zero gauge pressure and atmospheric temperature. Also, a constant heat flux input (1500W/m^2) is provided at the bottom of the plate to ensure uniform and constant heat flux. Four points on the surface of the plate are monitored during computation to observe the temperature variation across the plate during the simulation process.

In order to compare the dependency of Nusselt distribution curve on grid size, area averaged Nusselt number is calculated for different grid sizes. Of all the edges present, the edge containing (L1, L2) nozzle-target spacing and base length of the target surface is subjected to variation in the number of division. Different values of area averaged Nusselt number are recorded for different grid sizes, as shown in Table 1. Number of division on the edges L1 and L2 are varied from 300 to 550 and 125 to 400, respectively. Comparison of area averaged Nusselt number with its preceding value and experimental value define the most accurate grid size. This corresponding mesh consists of 550 × 400 numbers of divisions on edges L1 and L2 respectively (Figure 3).

Table 1 shows a comparison between the successive computed area averages Nusselt Number. Not only that, the computed value is also compared with the experimental value. This experimental value is determined at Re=10000 and Z/d=4. It is clear from Figure 3 that the mesh geometry with 550×400 numbers of divisions on edges L1 and L2 respectively, are the most appropriate choice.

As far as the flow profile and transition region at the target surface after the impingement is concerned, the commercial flow turbulence model available in the solver is not capable of predicting the Nusselt distribution accurately.

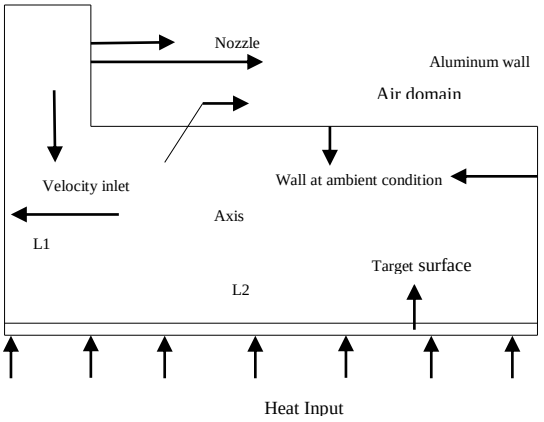

Figure 2. Schematic layout of axis symmetric computational geometry

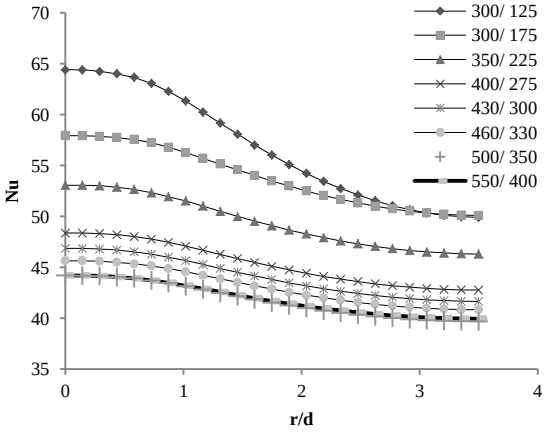

Figure 3. Nusselt Distribution curve for various numbers of divisions over edges L1 & L2

TABLE 1. Comparison of the area average Nusselt number at different grid sizes

Edge sizing		Nu_{avg}	%Deviation with preceding value	%Deviation with experimental value
Base (L1)	**Nozzle target (L2)**			
300	125	59.76	--	30.36%
300	175	53.83	10%	22.69%
350	225	49.46	8.1%	15.86%
400	275	45.38	8.2%	8.3%
430	300	44.08	2.87%	5.6%
460	330	43.09	2.23%	3.44%
500	350	42.48	1.41%	2.05%
550	400	41.92	1.32%	0.74%

The flow structure over the target surface after impingement consist of a stagnation region (0<r/d<1.0), transition region (1.0<r/d<2.5) and wall jet region (r/d>2.5) as described by Katti and Prabhu [17]. Hence, we need for a turbulence model which accurately records the temperature profile in the arena of near jet and wall jet region simultaneously. K-ε model is capable of well predicting the Nusselt distribution in stagnation region while K-ω model predicts well in wall jet region. On the other hand, SST model incorporates both the regions of flow regime and predicts accurate heat transfer dissipation as compared to K- ε and K-ω turbulence model. But the existence of transition region, intermediacy in flow profile and varying onset momentum based Reynolds number in the flow field, either promotes or degrades the Nusselt number. This phenomenon is not considered in any of the commercial CFX or FLUENT models. In order to consider the effect of heat transfer due the presence of intermediacy in flow profile and transition, Robin and Florian [9] proposed a transition model (Gamma – theta) which can be coupled to SST model in CFX solver. The benefit of this model lies in the accurate prediction of Nusselt number in the intervention period of intermediacy and transition. Figure 4 shows a variation of local Nusselt number with respect to radial distance for different turbulence model.

It can be seen from Table 2 that SST along with Gamma–Theta transition model shows a very close resemblance with experimental value. Not only this, the time required to attain the convergence of 10^{-8} using this model is approximately 2 hours, no to mention the 1.5 hour time required for achieving the steady temperature profile on experimental setup. However, the computational methodology are preferred on the effortless and accuracy grounds. K-Epsilon, K-Omega and SST turbulence models are not capable of predicting that accurate Nusselt profile. An error of 0.406% can be observed between experimental and computed value with use of SST along with two transition models.

Also, the present work takes an initiative in validating the present turbulence model with the results of Katti and Prabhu [17]. For this, the diameter of nozzle (13mm) and the dimension of target surface (104mm) are modified.

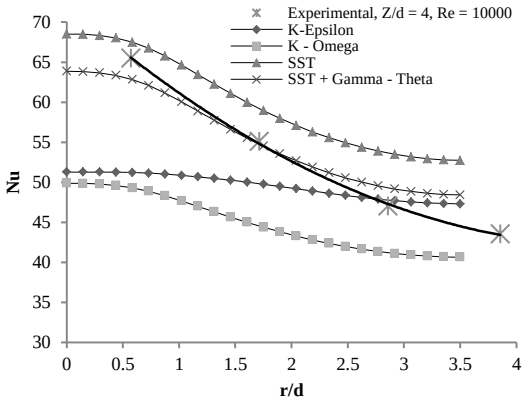

Figure 4. Nusselt distribution curve for different turbulence model

TABLE 2. Comparison of the average Nusselt number computed through different turbulence model.

Turbulence model.	Results for area averaged Nusselt number.		% deviation
--	Computation	Experiment	--
k – epsilon	49.5346	41.612	16%
k - omega	44.92596	41.612	7.37%
SST	59.96172	41.612	30.6%
SST+ Gamma-Theta	41.78259	41.612	0.406%

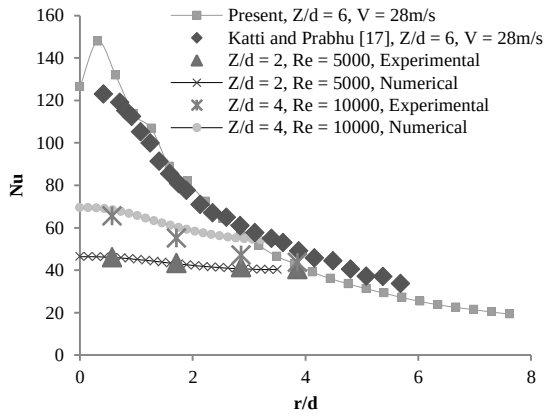

Figure 5. Validation of present Nusselt profile with the experimental and previous literature work

The comparison of Nusselt magnitude with previous work as shown in Figure 5 is done at Z/d=6 and impinging velocity of 28m/s. Not only this, the experimental profile evaluated at Z/d=2, 4 and Re=5000, 10000 are compared with the one computed using the present turbulence model. As far as the variation in geometric and injection parameter is concerned, the velocity of impingement and nozzle - target spacing are varied over the wide range as shown in Table 3. The local rise in Nusselt distribution curve is observed due to the presence of secondary peaks. These peaks are localized in stagnant and transition region. The intervening period for their occurrence solely depends upon the impinging Reynolds number and nozzle-target spacing.

However, the numerical constant which represents the probable occurrence of such peaks varies directly with impinging Reynolds number [17] and inversely with nozzle–target spacing (Z/d) [17]. The present work is inclined towards the determination of a critical magnitude of a non-dimensional number (Equation (8)), looking into which one can decide the occurrence of secondary peak in Nusselt distribution profile prior to the experiments.

The non-dimensional constant present in Equation (8) is evaluated by examining the value of Re (Z/d is fixed) above which the secondary peaks in the Nusselt profile starts occurring.

The magnitude of the constant reported using this approach is verified by determining the nozzle–target spacing (Re is maintained constant) above which the secondary peaks in the profile vanishes.

$$Constant\ (C) = \frac{Re}{Z/_d} \quad (8)$$

4. RESULTS

In order to determine the magnitude of non-dimensional constant, numerical results for local Nusselt number over the flat plate are evaluated at

i) Fixed nozzle-target spacing (Z/d=2) with varying Reynolds number.

ii) Fixed Reynolds number (Re=100000) with varying nozzle-target spacing.

TABLE 3. Ranges of injection and geometric parameters.

Parameters	Range
Velocity of jet	10 – 350 m/s
Z/d	5 – 30
Diameter of nozzle	7.35 mm
Area of base plate	100 × 100 mm^2
Heat input	15 Watts

In order to capture the origination of secondary peaks, the 2-D axis-symmetric model is computed at different inlet velocities, ranging from 10 to 350 m/s. The nozzle-target spacing is maintained constant (Z/d = 2) during this impingement condition. Figure 6 shows the origination of secondary peak in the Nusselt distribution curve occurring at velocity of 30m/s. Above this critical value with constant nozzle-target spacing, the appearance of secondary peaks becomes more remarkable and localized. Hence, the impingement velocity of 30m/s (Re=13230) is considered as a critical value in deciding the origination of secondary peaks. The corresponding non dimensional constant estimated at this condition round to 6615.

The diminishing point for the appearance of secondary peak is investigated at fixed impinging velocity (100m/s, Re=100000) and varying nozzle-target spacing. Obviously, the origination is computed at fixed spacing and increasing velocity. Figure 7 shows the plot of Nusselt distribution curve at constant velocity of 100 m/s and varying nozzle-target spacing. The variation in the spacing ranges from 5 to 30 times the diameter of nozzle. As seen from Figure 7, the secondary peak at higher spacing become small and diminishes at a particular critical instant (Z/d>15). The corresponding non dimensional constant as described in Equation (8) rounds to 6666, as far as the present approach is concerned.

Looking into the origination and diminishing points of secondary peaks in regards with the magnitude of non-dimensional constant (Equation (8)), the critical magnitude for the appearance of secondary peaks in Nusselt distribution curve can be approximately rounded to 6000. Above this value, occurrence of secondary peaks in Nusselt profile is certain.

The value of non-dimensional constant above which the possibility for the occurrence of secondary peaks exist, is investigated to be 6000. This is as per the present investigation. In order to validate this magnitude, Nusselt profile from the previous studies [17,19,20] was examined (Table 4).

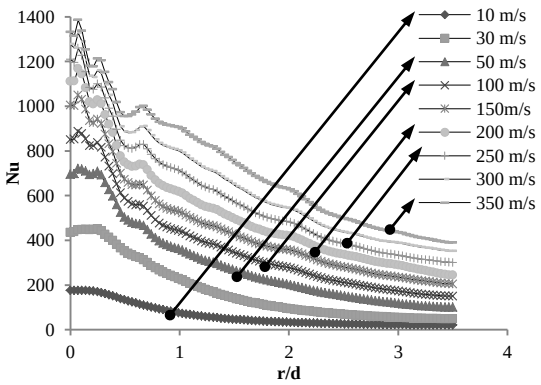

Figure 6. Variation of local Nusselt number at different velocity and constant jet to target spacing

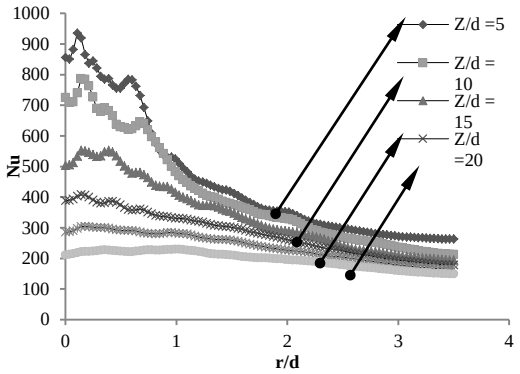

Figure 7. Variation of local Nusselt number at different nozzle - target spacing and fixed impinging velocity

TABLE 4. Validation of non-dimensional constant

Source	Z/d	Re	C	Secondary peak
Katti and Prabhu [17]	0.5	12000	24000	✓
Katti and Prabhu [17]	0.5	28000	56000	✓
Katti and Prabhu [17]	2	12000	6000	✗
Katti and Prabhu [17]	2	28000	14000	✓
Katti and Prabhu [17]	4	28000	7000	✓
Katti and Prabhu [17]	4	12000	3000	✗
Katti and Prabhu [17]	8	12000	1500	✗
Katti and Prabhu [17]	8	28000	3500	✗
Sajad et al. [20]	2	6000	3000	✗
Sajad et al. [20]	2	14000	7000	✓
Sajad et al. [20]	6	6000	1000	✗
Sajad et al. [20]	6	14000	2333	✗
Donovan et al. [21]	0.5	1000	20000	✓
Donovan et al. [21]	8	10000	1250	✗
Donovan et al. [21]	0.5	30000	60000	✓
Donovan et al. [21]	2	30000	15000	✓
Donovan et al. [21]	4	30000	7500	✓
Donovan et al. [21]	8	30000	3750	✗

However, the secret behind the occurrence of secondary peaks is the transition occurring in the flow regime over the target surface. In order to visualize this transition layer, velocity contours were mapped at different values of non-dimensional constant as shown in Figure 8.

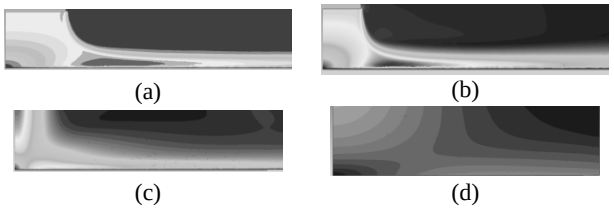

Figure 8. Velocity contour in near stagnation region for the non-dimensional constants of 10000 (a), 8000(b), 6000(c) and 4000(d)

5. CONCLUSION

The most accurate prediction of Nusselt profile is achieved with the use of SST + Gamma-theta turbulence model. Intermediacy and onset transition of Reynolds number are observed to be the most vital characteristic of air jet impinging over a flat target surface. The proposed 2-D computational geometry consumes the computational time of 2 hour to attain the overall convergence criteria of 10^{-8}. However, the appearance of secondary peaks in Nusselt profile is examined to exits when the value of non-dimensional constant exceeds 6000. The non-dimensional constant in the present research varies directly with the impinging velocity and inversely with nozzle-target spacing. Also, the contributions of both parameters in generation of the secondary peaks are on equal footings. The existence of such peaks increases the area average Nusselt magnitude. The mapping of velocity contours at different magnitudes of this non-dimensional constant justifies the occurrence of transition skin in the near wall region of the flow field. This transition skin stretches with the increase in magnitude of the non-dimensional constant. This stretched layer actually consists of many random velocity vectors whose magnitudes are almost equivalent to the potential core of impinging jet. Due to such turbulence occurring over the intermediate position of target surface, heat transfer rate locally increases for a small instance. This gives rise to a localized secondary peak. Actually, the occurrence of this turbulence anomaly in the near wall region ($r/d<2$) is due to an abnormal slip of vertical impinging velocity vectors with stagnation point. This type of slip generates a higher velocity gradient just adjacent to the stagnation region. Hence, the flow region which is adjacent to the stagnation point is under a strong turbulence behavior.

6. REFRENCES

1. El-Sheikh, H.A. and Garimella, S.V., "Heat transfer from pin-fin heat sinks under multiple impinging jets", ***IEEE Transactions on Advanced Packaging***, Vol. 23, No. 1, (2000), 113-120.
2. Garimella, S.V. and Schroeder, V.P., "Local heat transfer distributions in confined multiple air jet impingement", ***Journal of Electronic Packaging***, Vol. 123, No. 3, (2001), 165-172.
3. Yamane, Y., Ichikawa, Y., Yamamoto, M. and Honami, S., "Effect of injection parameters on jet array impingement heat transfer", ***International Journal of Gas Turbine, Propulsion and Power Systems***, Vol. 4, No. 1, (2012).
4. Lytle, D. and Webb, B., "Air jet impingement heat transfer at low nozzle-plate spacings", ***International Journal of Heat and Mass Transfer***, Vol. 37, No. 12, (1994), 1687-1697.
5. Choo, K.S. and Kim, S.J., "Heat transfer characteristics of impinging air jets under a fixed pumping power condition", ***International Journal of Heat and Mass Transfer***, Vol. 53, No. 1, (2010), 320-326.

6. Hikkimath, G.K. and Santosh S Chappar, "Numerical investigation of l/d ratio of nozzle on heat transfer characteristic of a circular jet on flat plate", ***Global Journal of Engineering Science and Researches***, (2014).
7. Huang, J.-B. and Jang, J.-Y., "Numerical study of a confined axisymmetric jet impingement heat transfer with nanofluids", ***Engineering***, Vol. 5, No. 01, (2013), 69-74.
8. Gorji, S., Seddighi, M., Ariyaratne, C., Vardy, A., O'Donoghue, T., Pokrajac, D. and He, S., "A comparative study of turbulence models in a transient channel flow", ***Computers & Fluids***, Vol. 89, (2014), 111-123.
9. Langtry, R.B. and Menter, F.R., "Correlation-based transition modeling for unstructured parallelized computational fluid dynamics codes", ***AIAA Journal***, Vol. 47, No. 12, (2009), 2894-2906.
10. Malan, P., Suluksna, K. and Juntasaro, E., "Calibrating the-re transition model for commercial cfd", ***AIAA Paper***, Vol. 1142, (2009).
11. Angioletti, M., Nino, E. and Ruocco, G., "Cfd turbulent modelling of jet impingement and its validation by particle image velocimetry and mass transfer measurements", ***International Journal of Thermal Sciences***, Vol. 44, No. 4, (2005), 349-356.
12. Alenezi, A., Teixeira, J. and Addali, A., "Numerical analysis of heat transfer characteristics of an orthogonal and obliquely impinging air jet on a flat plate", in Proceedings of the World Congress on Engineering. Vol. 2, (2015).
13. Khameneh, P.M., Mirzaie, I., Pourmahmoud, N., Rahimi, M. and Majidyfar, S., "A numerical study of single-phase forced convective heat transfer in tube in tube heat exchangers", ***World Academy of Science, Engineering and Technology, International Journal of Mechanical, Aerospace, Industrial, Mechatronic and Manufacturing Engineering***, Vol. 4, No. 10, (2010), 958-963.
14. Sundaram, M. and Venkatesan, M., "Heat transfer study of perforated fin under forced convection", ***International Journal of Engineering-Transactions A: Basics***, Vol. 28, No. 10, (2015), 1500.
15. Khoshravan, E. and Soleimani, G., "A numerical study of natural convection and radiation interaction in vertical circular pin", ***International Journal of Engineering***, Vol. 10, No. 3, (1997), 163-170.
16. Rostamzadeh, A., Jafarpur, K., Goshtasbirad, E. and Doroodmand, M., "Experimental investigation of mixed convection heat transfer in vertical tubes by nanofluid: Effects of reynolds number and fluid temperature", ***International Journal of Engineering-Transactions B: Applications***, Vol. 27, No. 8, (2014), 1251.
17. Katti, V. and Prabhu, S., "Experimental study and theoretical analysis of local heat transfer distribution between smooth flat surface and impinging air jet from a circular straight pipe nozzle", ***International Journal of Heat and Mass Transfer***, Vol. 51, No. 17, (2008), 4480-4495.
18. Chougule, N., Parishwad, G. and Sewatkar, C., "Numerical analysis of pin fin heat sink with a single and multi air jet impingement condition", ***International Journal of Engineering and Innovative Technology***, Vol. 1, No. 3, (2012), 44-50.
19. Alimohammadi, S., Murray, D.B. and Persoons, T., "Experimental validation of a computational fluid dynamics methodology for transitional flow heat transfer characteristics of a steady impinging jet", ***Journal of Heat Transfer***, Vol. 136, No. 9, (2014).
20. O'Donovan, T.S. and Murray, D.B., "Jet impingement heat transfer–part i: Mean and root-mean-square heat transfer and velocity distributions", ***International Journal of Heat and Mass Transfer***, Vol. 50, No. 17, (2007), 3291-3301.

On Numerical Investigation of Non-dimensional Constant Representing the Occurrence of Secondary Peaks in the Nusselt Distribution Curves

S. Mohd Umair, N. Parashram Gulhane

Department of Mechanical Engineering, Veermata Jijabai Technological Institute, Mumbai

P A P E R I N F O

Paper history:
Received 07 July 2016
Received in revised form 13 August 2016
Accepted 03 September 2016

Keywords:
Heat Transfer
Heat Sinks
Nusselt Number
Computational Simulations
Secondary Peaks

چکیده

ویژگی های نرخ پراکنش حرارتی به روش عددی و توزیع شعاعی بر روی سطح صاف به کمک عدد ناسلت ارزیابی گردید. در این تحقیق این پروفایل ها برای پارامترهای هندسی و جت های مختلف گزارش شده است. با نگرش متفاوت به این پروفایل ها، افزایش ناحیه ای و ثانویه اتفاق می افتد. چنین افزایشی به کمک عدد ناسلت قابل پیش بینی می باشد. در این تحقیق برای دسترسی به این اهداف، شبیه سازی عددی و محاسبات دامنه ای مشابه شزایط واقعی انجام شد. در شبیه سازی محاسباتی در فواصل کوناه نازل ها به سطح هدف، افزایش ثانویه در پروفایل عدد ناسلت اتفاق می افتد. ایجاد دامنه تداخل پیک های پروفایلی عدد ناسلت را نمی توان به خوبی مشاهده نمود. این تحقیق بر تعیین ضرایب ثابت بحرانی و اندازه پیک ها بر عدد ناسلت تمرکز نموده است. ضرایب ثابت بدون بعد نشانگر اندازه بحرانی است که می تواند با بکارگیری نسبت قطر بر عدد رینولدز پایه برای نازل و فاصله با سطح مورد نظر (Z/d) تعیین گردد. با ارزیابی پروفایل و کنتر سرعت، جریان توربولنت نزدیک ناحیه دیواره اتفاق افتاده که ماحصل آن موجب افزایش نرخ انتقال حرارت می شود.

***doi**: 10.5829/idosi.ije.2016.29.10a.14*